Variability of Tropical Cyclone Representation within Atmospheric Reanalysis Datasets

Ben Schenkel (bschenkel@fsu.edu) and Robert Hart (rhart@fsu.edu)
Department of Earth, Ocean, and Atmospheric Science, Florida State University

Introduction

The emergence of reanalyses has provided tools of great utility for studying interactions between tropical cyclones (TCs) and their larger scale environment. In spite of the increasing usage of reanalyses for climate scale studies of TCs, there has been no comprehensive examination of the representation of TCs within these datasets. The implications of the accurate depiction of TCs within reanalyses may have far reaching consequences including potentially impacting the representation of the general circulation on short time scales. The following study seeks to quantitatively compare reanalysis TC position, intensity, and structure with observational datasets and examine how these parameters vary within and among reanalysis datasets.

Methodology

In this study, the fidelity of TC position, intensity, and structure is examined within five reanalyses: the NCEP CFSR (Saha et al. 2010), the ECMWF ERA-40 (Uppala et al. 2005), the ECMWF ERA-I (Simmons et al. 2007), the JMA JRA-25 (Onogi et al. 2007), and the NASA MERRA (Bosilovich et al. 2006). TCs that are found equatorwards of 36°N within the NHC best-track dataset (Jarvinen et al. 1984; Neumann et al. 1993) and JTWC best-track dataset (Chu et al. 2002) in the eastern North Pacific, North Atlantic, and western North Pacific between 1979–2001 are chosen for study. Each best-track TC within the reanalysis is manually tracked using minimum mean sea-level pressure and maximum 925 hPa relative vorticity. The reanalysis position and intensity are then compared to those found in the best-track dataset.

In addition to examining these traditional metrics, parameters from the cyclone phase space (Hart et al. 2003) and storm-relative composites of anomalies are used to evaluate TC structure. The composites are constructed by bilinearly interpolating each grid to a uniform horizontal resolution centered about the manually tracked reanalysis TC position. Each reanalysis TC is then composited into one of four intensity bins according to its best-track intensity.

Spatial Variation of Tropical Cyclone Position Difference

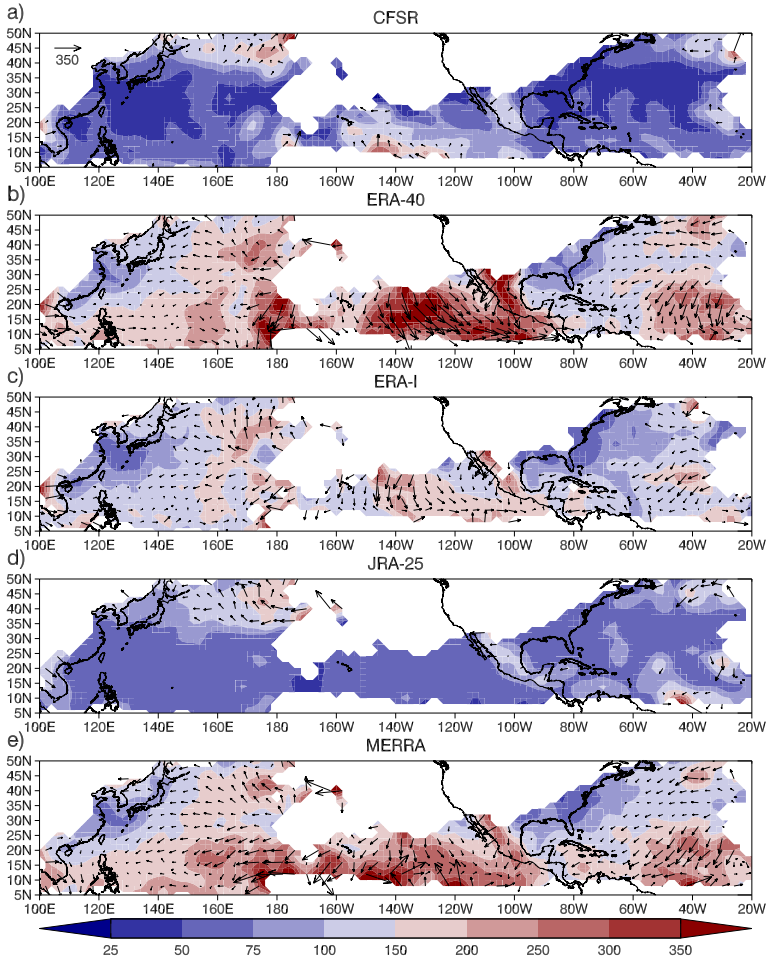

Figure 1: Plan view of the mean position difference (km) magnitude (shaded) and vector displacement (arrow, reanalysis position relative to best-track) for the (a) CFSR, (b) ERA-40, (c) ERA-I, (d) JRA-25, and (e) MERRA for TCs in the eastern North Pacific, North Atlantic, and western North Pacific. The mean magnitude of the position differences is interpolated to a 2° by 2° grid representing the average of the position difference weighted by its distance from the gridpoint. For clarity, the vector displacement of the position difference is interpolated to a 4° by 4° grid with vectors excluded for gridpoints with values of less than 100 km. The grid is smoothed once with a nine-point smoother.

Mean Tropical Cyclone Position and Intensity Differences

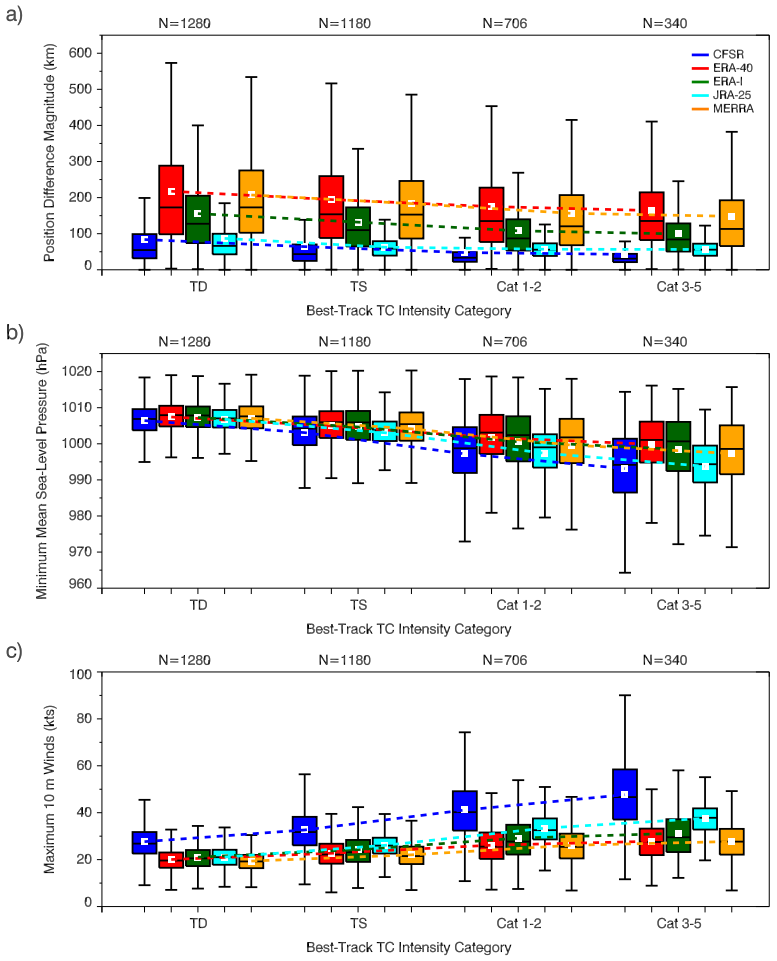

Figure 2: Box and whiskers plot of (a) position difference magnitude (km), (b) minimum mean sea-level pressure (hPa), and (c) maximum 10 m winds (kts) for the eastern North Pacific, North Atlantic, and western North Pacific for each of the five reanalyses stratified by the four best-track intensity categories used in this study. The CFSR, ERA-40, ERA-I, JRA-25, and MERRA correspond with color coding of blue, red, green, cyan, and orange respectively. The mean of the sample is denoted by a white square printed within each box. The number of distinctly named TCs for each intensity bin is denoted at the top of each figure. The dashed lines connect the mean of each intensity bin for each reanalysis in order to help identify trends within datasets.

Variability of Tropical Cyclone Representation within Atmospheric Reanalysis Datasets

Ben Schenkel (bschenkel@fsu.edu) and Robert Hart (rhart@fsu.edu)
Department of Earth, Ocean, and Atmospheric Science, Florida State University

Spatial Variation of Low-Level Tropical Cyclone Structure

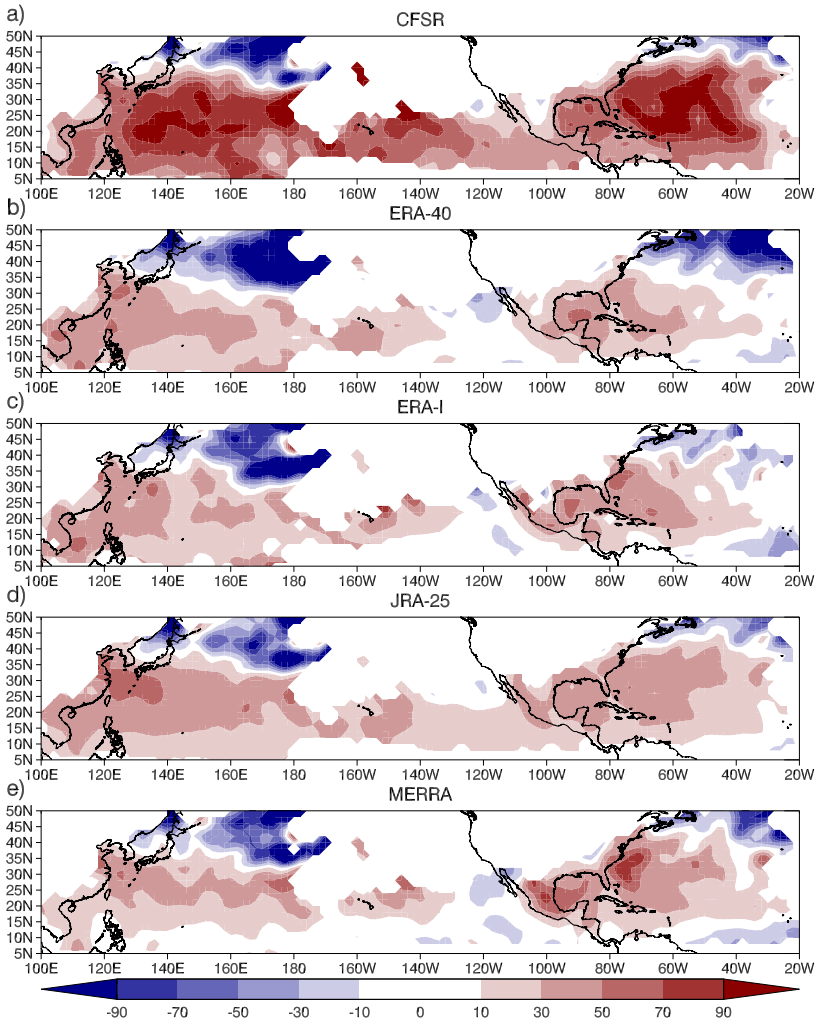

Figure 3: Plan view of the mean low-level thermal wind (calculated between 900 hPa and 600 hPa) from the cyclone phase space for the (a) CFSR, (b) ERA-40, (c) ERA-I, (d) JRA-25, and (e) MERRA for TCs in the eastern North Pacific, North Atlantic, and western North Pacific. Mean low-level thermal wind is interpolated to a 2° by 2° grid representing the average of the low-level thermal wind weighted by its distance from the gridpoint. The grid is smoothed once with a nine-point smoother.

North Atlantic Category 3–5 Tropical Cyclone Structure in Reanalyses and Observations

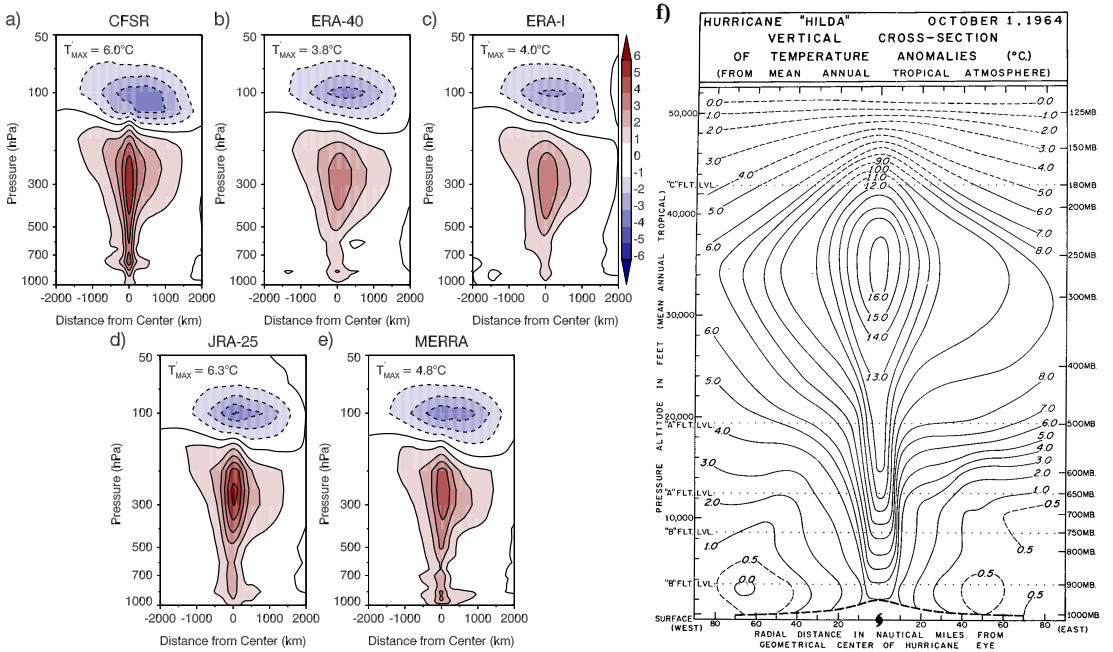

Figure 4: Vertical cross-section of composited storm-relative temperature anomalies (°C) in the (a) CFSR, (b) ERA-40, (c) ERA-I, (d) JRA-25, and (e) MERRA for North Atlantic category 3–5 TCs. (f) Vertical cross-section of storm-relative temperature anomalies for TC Hilda on October 1, 1964 (Hawkins and Rubsam 1968).

Discussion

The results of this study show that reanalysis TC representation exhibits significant variability among basins. Specifically, North Atlantic TCs have the smallest position differences, strongest intensities, and largest composited anomaly magnitudes. The robust representation of North Atlantic TCs is likely attributable to a relatively greater density of observations. In contrast, eastern North Pacific TCs have the largest position differences, weakest intensities, and smallest composited anomaly magnitudes. The poorer representation of eastern North Pacific TCs is possibly due to the smaller mean size of TCs relative to other basins (Chavas and Emanuel 2010; Schenkel and Hart 2011) and a relative dearth of observations (Hatsushika et al. 2006; Manning 2007; Vecchi and Knutson 2008). Artificial trends in reanalysis TC representation are also seen likely due to variations in the density of observations, observed TC age, observed TC size, and the resolution of the reanalysis. Among the reanalyses, the most realistic representation of TCs is found within the CFSR and JRA-25 due to the use of vortex relocation (Liu et al. 2000) and TC wind profile retrievals (Hatsushika et al. 2006), respectively. While the coarse resolution of reanalyses precludes the replication of the observed intensity of TCs, the gross structure of TCs is captured reasonably well. Given the particularly poor representation of the strongest intensity TCs, caution should be exercised when utilizing these datasets for calculations dependent on resolving the absolute magnitude of quantities such as TC intensity metrics.

Acknowledgments and References

This research is supported by NASA Headquarters under the NASA Earth and Space Science Fellowship Program Grant 10-Earth10R-0036 and NSF Grant ATM-0842618. The authors also would like to thank Michael Bosilovich (NASA GSFC) for fruitful discussions regarding MERRA. We acknowledge the FSU HPC facility and staff for contributions to the results presented in this poster.

Bosilovich, M., and Coauthors, 2006: NASA's Modern Era Retrospective-Analysis for Research and Applications (MERRA). *Geo. Res. Abstracts*, **8**, 05160.
Chavas, D. and K. Emanuel, 2010: A QuikSCAT climatology of tropical cyclone size. *Geophys. Res. Lett.*, **37**, L18816.
Chu, J., C. Sampson, A. Levine, and E. Fukada, 2002: The Joint Typhoon Warning Center Tropical Cyclone Best-Tracks, 1945–2000. *Naval Research Laboratory,Reference Number NRL/MR/7540-02-16*.
Hart, R., 2003: A Cyclone Phase Space Derived from Thermal Wind and Thermal Asymmetry. *Mon. Wea. Rev.*, **131**, 585–616.
Hatsushika, H., J. Tsutsui, M. Fiorino, and K. Onogi, 2006: Impact of Wind Profile Retrievals on the Analysis of Tropical Cyclones in the JRA-25 Reanalysis, *J. Meteor. Soc. Japan*, **84**, 891–905.
Hawkins, H. and D. Rubsam, 1968: Hurricane Hilda, 1964. *Mon. Wea. Rev.*, **96**, 617–636.
Jarvinen, B., C. Neumann, and M. Davis, 1984: Tropical Cyclone Data Tape for the North Atlantic Basin, 1886–1983: Contents, Limitations and Uses. *NOAA Tech. Memorandum NWS NHC-22*.
Liu, Q., T. Marchok, H. Pan, M. Bender, and S. Lord, 2000: Improvements in hurricane initialization and forecasting at NCEP with global and regional (GFDL) models. NOAA Technical Procedures Bulletin, **472**.
Manning, D., 2007: The Utility of the ERA40 Cyclone Phase Space in Trend Diagnosis and North Atlantic Tropical Cyclone Reanalysis. M.S. thesis, The Florida State University, Tallahassee, FL 32303, 79 pp.
Onogi, K. and Coauthors, 2007: The JRA-25 Reanalysis. *J. Meteor. Soc. Japan*, **85**, 369–432.
Saha, S. and Coauthors, 2010: The NCEP climate forecast system reanalysis. *Bull. Amer. Meteor. Soc.*, **91**, 1015–1057.
Schenkel, B. and R. Hart, 2011: An Examination of Tropical Cyclone Position and Intensity Differences within Atmospheric Reanalysis Datasets. *J. Climate*, **conditionally accepted**.
Uppala, S., S. Uppala, D. Dee, and S. Kobayashi, 2007: ERA-Interim: New ECMWF Reanalysis Products from 1989 Onwards. *ECMWF Newsletter*, **110**, 25–35.
Uppala, S. and Coauthors, 2005: The ERA-40 Reanalysis. *QJRMS*, **131**, 2961–3012.
Vecchi, G. and T. Knutson, 2008: On Estimates of Historical North Atlantic Tropical Cyclone Activity. *J. Climate*, **21**, 3580–3600.